Research on the Application of a 3-m Transmitter Loop for TEM Surveys in Mountainous Areas

Guo-qiang Xue[1,*], Nan-Nan Zhou[1], Wei-ying Chen[1], Hai Li[1] and Shu Yan[2]
[1]Key Laboratory of Mineral Resources, Institute of Geology and Geophysics, Chinese Academy of Sciences, Beijing 100029, China
[2]School of Computer Science and Telecommunication Engineering, Jiangsu University, Zhenjiang 212013, China, Tel: +86-511-88797508
*Email: ppxueguoqiang@163.com; Tel: +86-10-82998193

ABSTRACT

Large loop transient electromagnetic (TEM) is a widely used surface exploration method for mapping electrically conductive bodies. However, when working in the mountainous areas of China, it is difficult to lay out large enough transmitter loops for conventional surveys. An option for this type of terrain is a newly designed TEM survey configuration that uses a small 3-m square loop in combination with a high current (1,000 A to 2,000 A) TEM transmitter to excite a powerful EM field for detecting targets at greater depths. The detection depth of the system is analyzed. After comparing the responses as well as the detection depths between this special system and standard large loop configurations, it is shown that: 1) a small loop system can result in a detection depth similar to that of a large loop system; and 2) a small loop system is superior to a large loop during shallow depth target detection as well as in mountainous areas. Sufficient signal intensity can be obtained by a small central loop configuration equipped with a high current transmitter and a large equivalent area receiver coil. A large trial survey was conducted on the surface of mountainous areas in the Shanxi Province of China. This TEM survey showed that the 3-m by 3-m transmitter loop system was an effective method for deep TEM sounding in mountainous areas.

Introduction

The transient electromagnetic (TEM) technique is a common surface-based geophysical method that provides resistivity information about the subsurface. Large loop, central loop and coincident loop (Raiche and Gallagher, 1985) TEM surveys have been widely used in mineral exploration, engineering, and environmental investigation as well as miscellaneous geologic studies (Singh *et al.,* 2009; Beard, 2011; Xue *et al.,* 2012a, b).

The purpose of using large transmitter loops in TEM surveys is to maintain a high signal-to-noise ratio. However, Spies (1980, 1989) reached the conclusion that the major factor influencing the depth of penetration was the sample time, not the loop size. When working in the mountainous areas of China, it is difficult to lay out large enough transmitter loops for conventional surveys. Since 1993, the equipment and technology for a small-scale and high current transmitter loop system has been developed for deep exploration in such mountainous areas. A large number of case histories with this system have been conducted in China, but only a few have been published. Based on numerical simulations, a new small loop configuration was presented by Guo *et al.* (2010) and Xue *et al.* (2012c). Their system uses a 3-m transmitter loop for mapping of tunnels up to depths of 30 m. Conducting TEM soundings with a 5-m square loop was discussed by Yan *et al.* (2009a). They studied the diffusion of TEM fields into a two-dimensional (2-D) earth, simulated by a finite-difference time-domain (FDTD) algorithm, and whether a small loop configuration could be used for greater depth of investigation and higher resolution exploration. It is worthwhile further researching the performance of this special system.

In this study, the detection depth and response of a small loop system were compared with that of a large loop configuration. In addition, field examples for coal mine water-filled zone investigations are presented, in which a 3-m by 3-m loop was used in mountainous areas near Linfen City, Shanxi Province, China. The field results and interpretations from this study are reported herein exploring hidden extensions of mined-out coal seams and searching for water-enriched areas.

 DOI: 10.2113/JEEG19.1.3

Responses of Small Loop and Large Loop TEM Configurations

With the assumption of a layered earth, the surface response of a circular loop in the frequency domain can be expressed as (Spies, 1980; Kaufman and Keller, 1983; Nabighian and Macnae, 1991):

$$H_z(\omega) = I_0 a \int_0^\infty \frac{\lambda Z^{(1)}}{Z^{(1)} + Z_0} J_1(\lambda a) J_0(\lambda r) d\lambda, \quad (1)$$

or

$$\frac{dB_z(\omega)}{dt} = -i\omega\mu_0 I_0 \int_0^\infty \frac{\lambda Z^{(1)}}{Z^{(1)} + Z_0} J_1(\lambda a) J_0(\lambda r) d\lambda, \quad (2)$$

where I_0 denotes the transmitter current in a circular loop, λ denotes the variable of integration, Z_0 denotes the surface impedance, $Z^{(1)}$ denotes the total impedance of the earth, r is the distance from the center of the loop to the field point, and a is the radius of the circular loop. The time-domain step response of large circular loops is given as:

$$H_z(t) = \frac{2}{\pi} \int_0^\infty \mathrm{Im} \left[I_0 a \int_0^\infty \frac{\lambda Z^{(1)}}{Z^{(1)} + Z_0} J_1(\lambda a) J_0(\lambda r) d\lambda \right] \frac{\cos \omega t}{\omega} d\omega, \quad (3)$$

or

$$\frac{dB(t)}{dt} = \frac{2}{\pi} \int_0^\infty \mathrm{Re} \left[I_0 a \int_0^\infty \frac{\lambda Z^{(1)}}{Z^{(1)} + Z_0} J_1(\lambda a) J_0(\lambda r) d\lambda \right] \cos \omega t d\omega, \quad (4)$$

where t is the time. The responses were calculated according to Eq. (3) for three circular loops with radii a = 200 m, 100 m, and 50 m (to simulate large loops). The model parameters include ρ_1 = 10 Ω-m, ρ_2 = 20 Ω-m, and h_1 = 100 m. To simulate small loops, responses were calculated for the cases of a = 10 m and 3 m. All the loops use the same magnetic moment (product of area and current) of 9,000 m^2-A. The calculated results are shown in Fig. 1, where the horizontal axis is the time, and the vertical axis is the magnetic response. The corresponding loop radius and current parameters are listed in Table 1.

Figure 1(a) shows five magnetic response decay curves corresponding to the five loop radii of a = 200 m, 100 m, 50 m, 10 m and 3 m. Figure 1(b) shows five apparent resistivity curves corresponding to the same five loop radii. It is shown that: 1) within 2 ms time delay, the response from the small loop model is higher

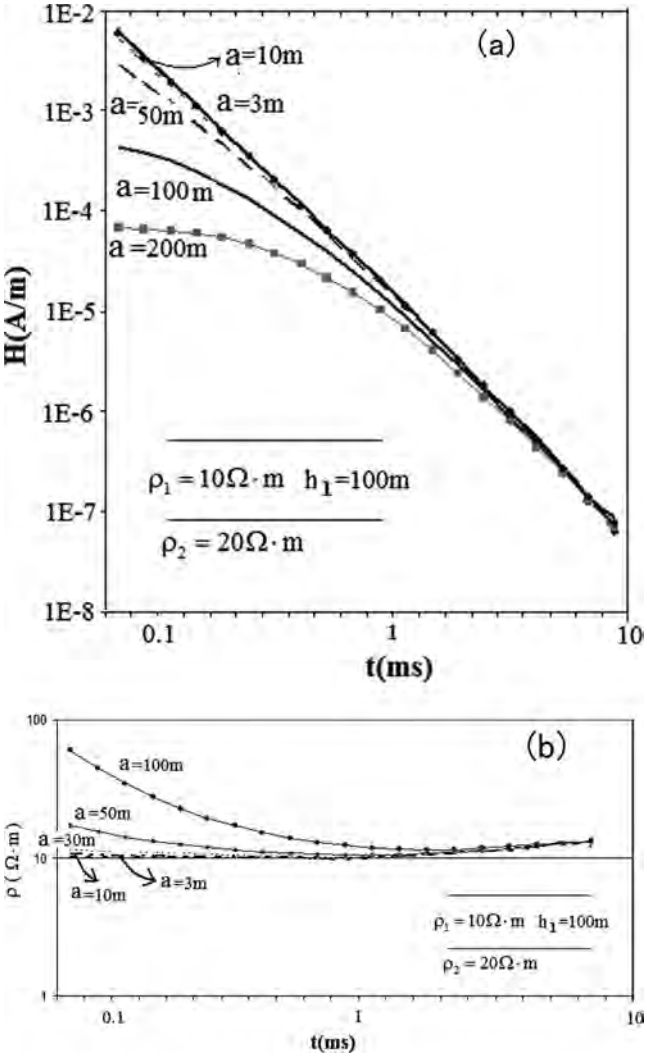

Figure 1. Model responses for the same magnetic moment (9,000 m^2-A), but different loop radii (a = 200 m, 100 m, 50 m, 10 m, and 3 m). a) Magnetic field decay curves; b) apparent resistivity curves.

Table 1. Transmitter loop parameters resulting in a 9,000 m^2-A magnetic moment.

a (m)	I (A)
500	0.36
200	0.225
100	0.9
50	3.6
10	90
3	1,000

than for the large loop model (Fig. 1(a)), which means a small loop is more suitable for shallow detection; 2) in the late time, the responses of the five different size loops are consistent, *i.e.*, theoretically, all of them have the same deeper depth of interrogation as expected; and 3) small loop sources are more sensitive to shallow targets.

Comparison of the Diffusion Depth between Small and Large Transmitter Loop Configurations

The following equation was proposed to estimate the diffusion depth D(t) of TEM fields by Spies (1989):

$$D(t) = \sqrt{\frac{\rho \cdot t}{2\mu_0}}. \quad (5)$$

where ρ is the earth resistivity and μ_0 is the permeability of free space. Equation (5) clearly shows that the investigation depth of TEM is primarily determined by the measurement time and earth resistivity, not by the loop size (Spies, 1989).

To verify this finding, a 2-D model was created with a conductive overburden and an anomalous body using a FDTD algorithm (Oristaglio and Hohmann, 1984; Wang and Hohmann, 1993). In this computation, the separation between sides of the 2-D loop is 200 m to simulate a large loop and 3 m for a small square loop. The measurement time is 3 ms and the transmitter current is 1 A. Boundary conditions for the model were treated in the same way as in the studies conducted by Oristaglio *et al.* (1984). The surface-air boundary is treated based on approximate quasi-static conditions; the bottom boundary and side boundaries, which are far away from the anomalous body, are treated using absorbing boundary conditions.

The results are shown in Fig. 2. It can be seen that the field response curves of both large (a) and small (b) loops with equal depth and time are similar in shape. Thus, if a larger transmitter current can be provided (I_0 = 1,200 A to 2,000 A), a small loop might be able to detect targets at the same depth (for example 200 m) as can be achieved using large loops, assuming that the signal-to-noise ratio is favorable and the receiver has enough resolution to pick up the lower signals.

Comparison of Depth of Investigation between Small and Large Loop Configurations

Although the TEM diffusion depth mainly depends on diffusion time, it is difficult to quantify the investigation depth because of many factors, such as signal-to-noise ratio. Considering the lump-sum effect of these factors, the depth of investigation was also proposed by Spies (1989):

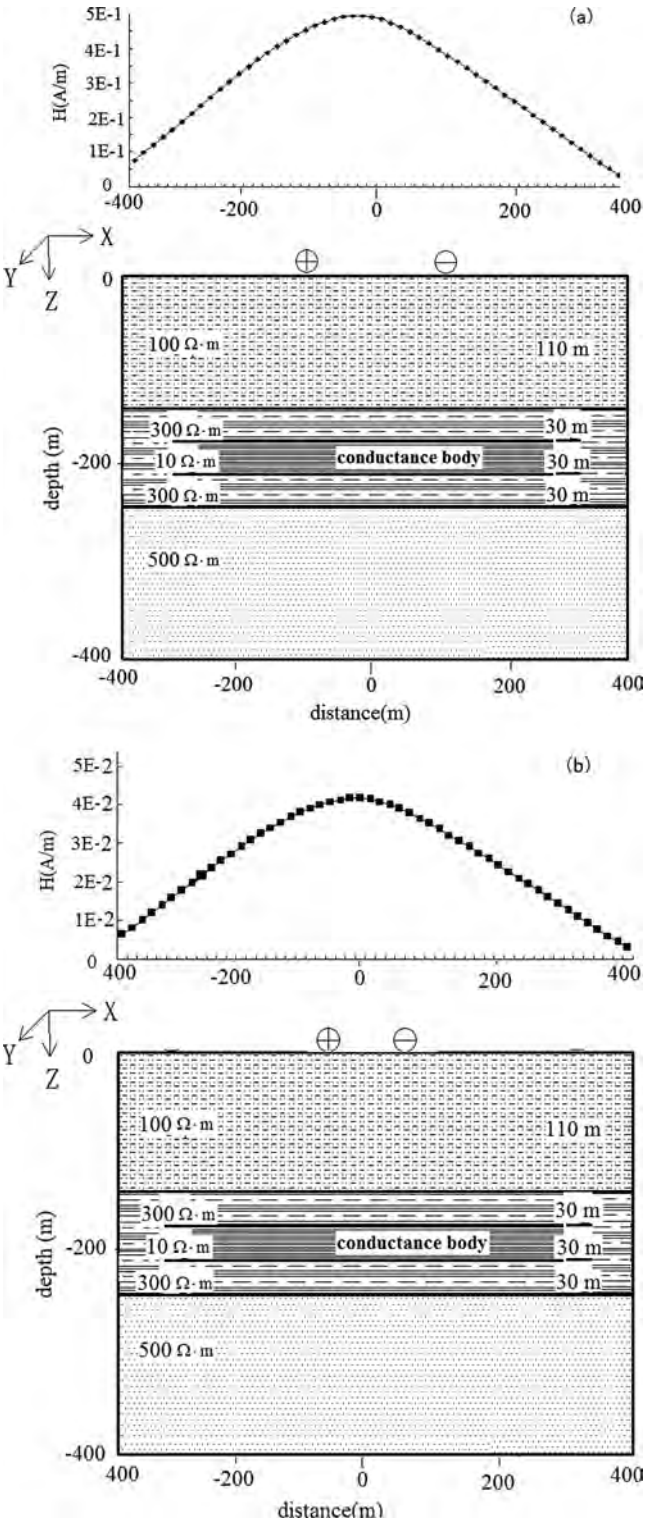

Figure 2. Subsurface magnetic fields (in A/m) at t = 3 ms for a large and small transmitter loop, both with 1-A transmitter current. (a) The separation between sides of the transmitter loop is 200 m. (b) The separation between sides of the loop is 3 m. Electrical model parameters are $\rho_1 = 100$ Ω-m, $\rho_2 = \rho_4 = 300$ Ω-m, $\rho_3 = 10$ Ω-m, and $\rho_5 = 500$ Ω-m.

Table 2. Comparison of parameters described in Eq. (6).

a (m)	η_v (nV/m^2)	σ_1 (Ω-m)	I (A)	d (m)
466	0.20	50	12	800
3	0.20	50	28,937	800
5	0.20	50	10,417	800
144	0.30	50	12	500
3	0.30	50	4,139	500
5	0.30	50	1,490	500
31	0.40	100	10	300
3	0.40	100	214.5	300
5	0.40	100	77.2	300
2	0.50	100	10	100
3	0.50	100	1.1	100
5	0.50	100	0.30	100

Table 3. Specifications of the EMRS-3 system.

Parameter	Description
Transmitter current	1,800 A
Transmitter loop size	3 m × 3 m
Receiver loop size	3 m × 3 m, 6 turns (or magnetic probe)
Total gain	16,384 times
Dynamic range	140 db
Time delay range	80 μs to 32 ms
Transmitter pulse width	32 μs
Time windows	22
Resolution	0.1 μV
Receiver bandwidth	0–20 KHz
Sampling rate	80 μs

$$d(t) \approx 0.55\left(\frac{I_0 A}{\sigma_1 \eta_v}\right)^{1/5}, \qquad (6)$$

where I_0 is the current, A is the transmitter area, σ_1 is the average conductivity of overlying strata, and η_v is the minimum distinguishable voltage. Using Eq. 6 and assuming a target depth of investigation of d(t) = 800 m with σ_1 = 0.02 S/m, I_0 = 12 A, η_v = 20 nV/m^2, the required side length for a square transmitter loop would be 465 m.

In Table 2, it is clearly shown that the depth (d(t) = 500 m) of a large loop (a = 144 m) with a 12 A current is equivalent to that of a small loop source (a = 5 m) with 1,490 A. Thus, the conclusion can be reached that it is theoretically feasible to use a small loop source for the investigation of deep geological bodies. With the instrumentation described herein, the transmitter current can be up to 2,000 A using a 3-m × 3-m small loop and reach a depth of 300 m.

The EMRS-3 TEM High Current System

Figure 3 shows a diagram (left) of the TEM instrument and its components (right). The system can be used to detect 50–500 m deep buried targets. A special capacitor is charged until its voltage reaches 1,000 V. Then the capacitor is discharged abruptly to deliver a high current (usually 1,800 A) to the transmitter loop. The transmitter loop is made of a special large-diameter wire (300 mm) with a resistance (per 100 m) of less than 0.5 Ω-m.

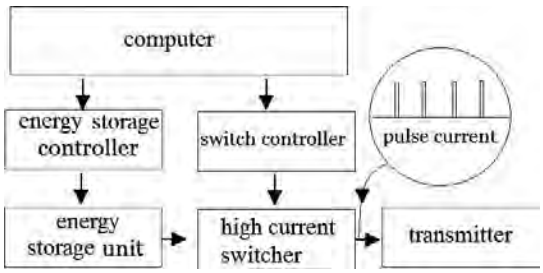

Figure 3. Main system diagram of the EMRS-3 TEM system.

The key components of the EMRS-3 system are the transmitter system and the receiver system. The transmitter system includes an energy storage unit and a high current switcher. The energy is charged in a capacitor that discharges a high current, which is controlled by the switcher. A positive transmitter step-current (1,800 A) is generated in the loop, the capacitor is recharged, the next positive step current is applied, and the cycle repeats. To improve the quality of observed data, a multi-transmitting function can be used. The number of transmitting pulses (1, 4, 8, and 16) is selected by the user. The transmitter turn-off time is 80 μs. The receiver system has 22 time gates with a selectable time delay range of 80 μs to 32 ms. Table 3 lists the specifications of the EMRS-3 system.

The system operational steps are shown in Fig. 3. After receiving instructions from the system computer, the energy storage unit begins to store energy. Next, the current switcher begins sending high current to the transmitter and then the induced signal is measured using either a magnetic core or receiver loop (same loop as transmitter loop).

Figure 4 shows the system used in the field, which emphasizes the relatively small size of the transmitter/receiver coil and overall system. The system advantages are described as small size, light weight, large current, and the ability to be operated in a mountainous area in addition to areas with high electrical noise.

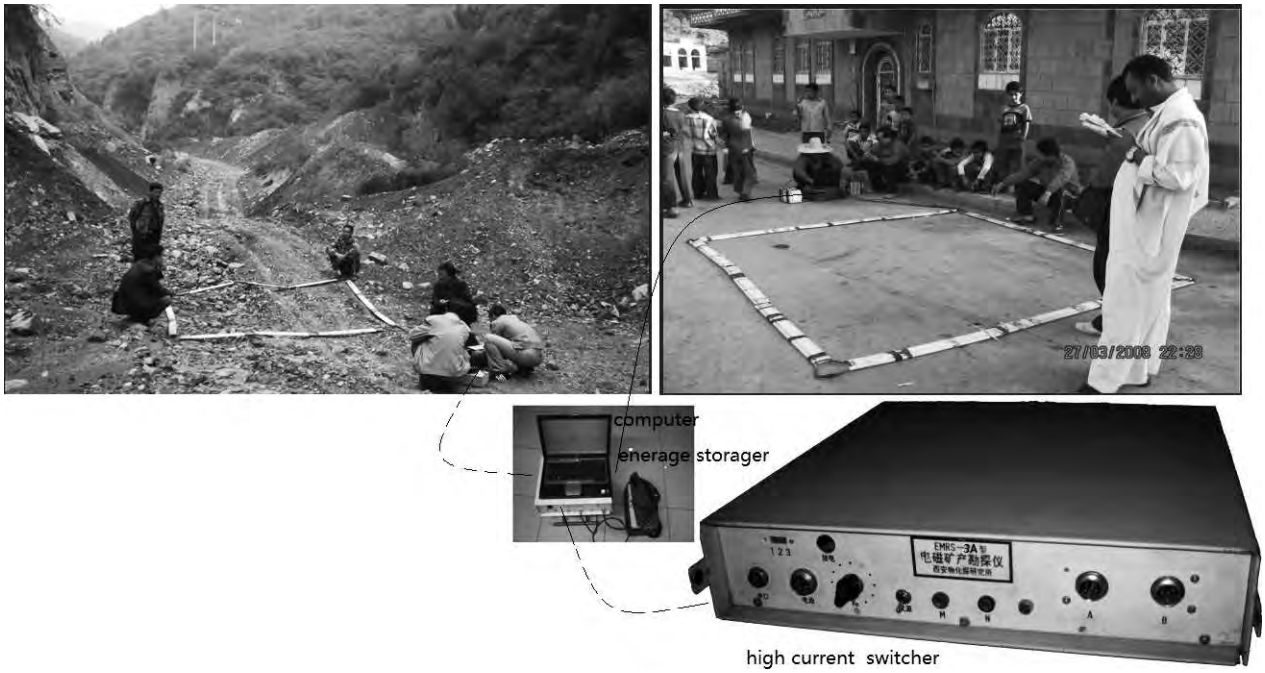

Figure 4. Picture of EMRS-3 system setup during field surveys.

Field Examples

There have been problems in coal mining operations in Shanxi Province of China caused by water rushing in (flooding), gas explosions, and collapses. Hence, it is necessary to identify any subsurface water sources that could topple columns during a mining operation and comprise mine safety. For these reasons, a TEM survey was conducted in the region.

The survey region is located in central Shanxi Province (Fig. 5). The primary purpose is to delineate the water-enriched areas in the coal-bearing strata. The geological sequence (in ascending order) in the survey area is comprised of the Ordovician Majagou Group, Carboniferous Benxi and Taiyuan Group, Permian Shanxi and Xiashihezi Group, and Cenozoic sediments (Table 4). Resistivity values for the sandstone, mudstone and coal strata ranges from 40 to 360 Ω-m. Limestone has a relatively high resistivity (>500 Ω-m). Because of the non-uniform distribution of water-enriched components between the top and bottom of the coal-bearing strata and the presence of cracks and faults, electrical properties change quickly, resulting in volumes of low resistivity. Resistivity values obtained from logging data of the various strata are given in Table 4. Water-filled voids exhibit a lower resistivity than host rocks.

The survey area is mountainous with an average elevation of about 1,387 m and relative height difference of 342 m; the topography is extreme (Fig. 5). It is difficult to lay out a 200 m side length loop for TEM exploration in this area. Hence, a small loop source TEM system (3 m × 3 m) was selected to conduct the surveys.

Field data were collected in a water-rich coal mining area using the EMRS-3 small-loop TEM system (Fig. 4, Table 3) developed by Xi'an Geophysical and Geochemical Exploration Institute. The surveyed data reading are in V(t)/I in units of μV/A:

$$\frac{\dot{B}(t)}{I} = \frac{dB(t)}{Idt} = V(t)/qI, \tag{7}$$

where q is the area of the receiver coil.

The following acquisition parameters were selected: a transmitter loop with side lengths of 3 m, a transmitting frequency of 25 Hz, a time-window range between 0.087–10 ms, and 20 time gates (Table 5).

The actual survey layout is shown in Fig. 6, showing a grid of 40 m by 10 m. It can be seen from Fig. 6 (bottom right picture) that this area is characterized by complex mountain topography. Data were acquired along 39 survey lines, with a line spacing of 40 m and a cumulative line length of 13.7 km. The distance between each measurement point was 10 m, corresponding to a total of 2,377 receiver locations.

To ensure the reliability of the EMRS-3 TEM system, preliminary transient sounding data were collected repeatedly at the same location. Figure 7(a) shows the TEM data collected five times at the same location. The decay curves are consistent, which means

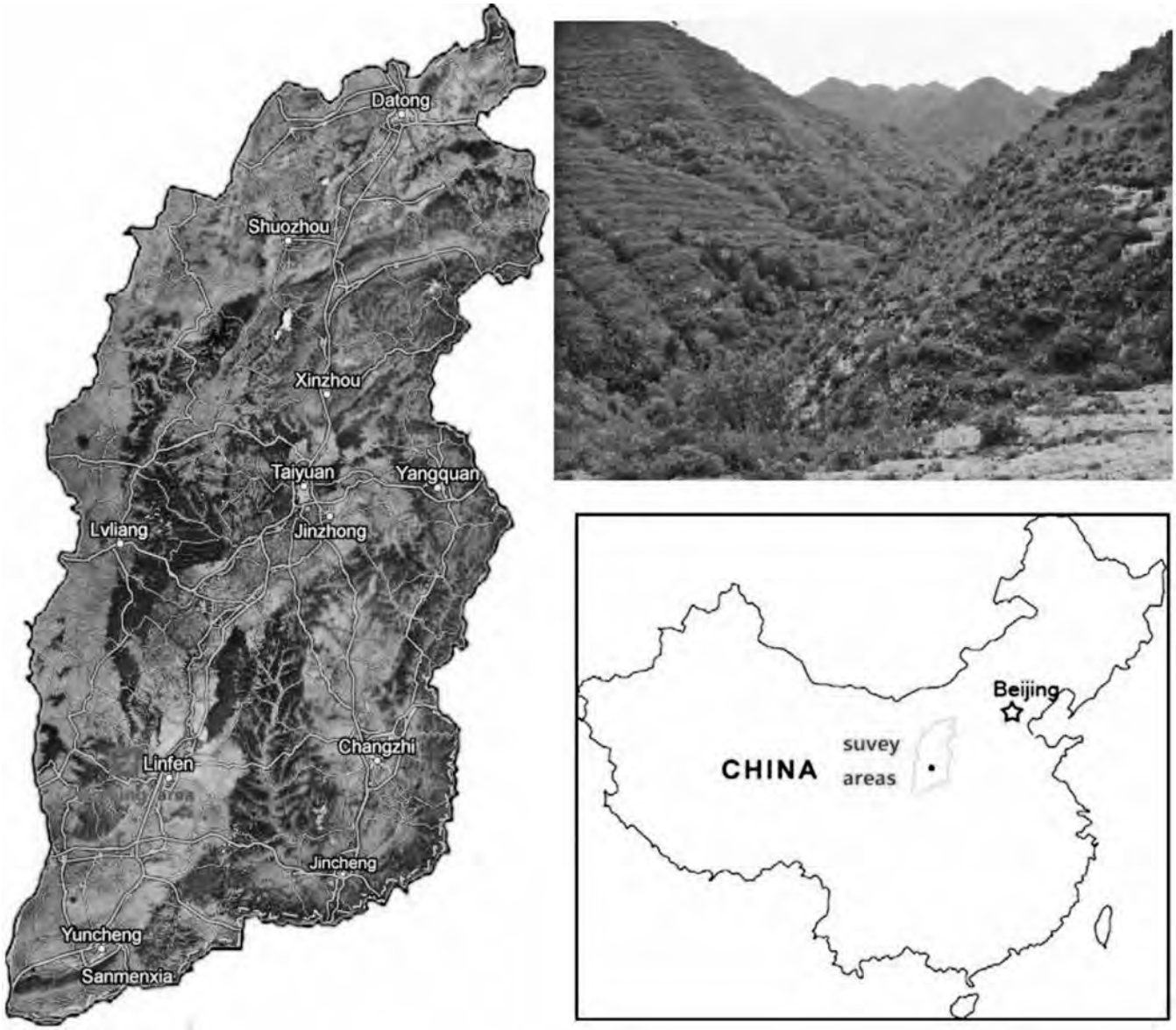

Figure 5. Maps of the working areas. Map of China indicating Shanxi province (lower right), Shanxi province (left), and an enlarged map of the local survey area in mountainous terrain (upper right).

Table 4. Resistivities of the different rock units in the survey region.

Geological age	Rock type	Resistivity (Ω-m)
Quaternary	Loess, clay, silt	16–50
Tertiary	Sand clay	40–100
Permian	Mudstone, siltstone	10–80
Carboniferous	Coal, thin limestone	70–360
Ordovician	Thick limestone	>500

that the EMRS-3 TEM system operation is stable and data are repeatable.

It is necessary to compare a traditional loop system with the 3 m by 3 m system. The comparison was conducted at a site having flat ground and known electrical characteristics. For a traditional system, the Australian-made Terra TEM system was selected, using a 100 m by 100 m loop with an input voltage of 24 V and a output current of 6 A. Figure 7(b) compares the decay curves collected with the Terra TEM and EMRS-3 systems. It is clearly shown that for the same geo-electric earth, the EMRS-3 system can achieve a satisfactory result and a small loop with high current configuration can be used for such TEM soundings.

Table 5. Time delay of time gates.

Gate number	1	2	3	4	5	6	7	8	9	10
Time (ms)	0.087	0.11	0.1381	0.219	0.2762	0.348	0.438	0.5524	0.696	0.877
Gate number	11	12	13	14	15	16	17	18	19	20
Time (ms)	1.105	1.392	1.7074	1.954	2	2.784	3.507	4.4193	5.568	7.015

An example of typical EMES-3 TEM decay curves collected during this study is given in Fig. 8(a). The data were acquired along line 10 at points 90 and 210 (refer to Fig. 6). The curve of point 90 exhibits a slow decay and is interpreted as a water-rich point, whereas the curve of point 210 exhibits a faster decay and is interpreted as a normal layered earth point.

Figure 8(b) shows the apparent resistivity contour section for line 10 and the corresponding interpreted geological result. The apparent resistivity ρ_τ (t) is calculated using (Kaufman and Keller, 1987):

$$\rho_\tau(t) = \frac{\mu_0}{4\pi t}\left(\frac{2\mu_0 Mq}{5tV(t)}\right)^{2/3}, \qquad (8)$$

where M represents the transmit magnetic moment, q presents the receiving area, and V(t) is the measured voltage. The depth is estimated using Eq. 5. It is clearly shown that three relatively low resistivity anomalies (120-200 Ω-m) exist at points 190, 320, and 420 with altitudes between 1,240 m and 1,140 m and a dip angle of 10°. The water-filled mine cavities at 0 m, 300 m to 330 m, and 400 m to 460 m have been marked by the dash line in the resistivity section.

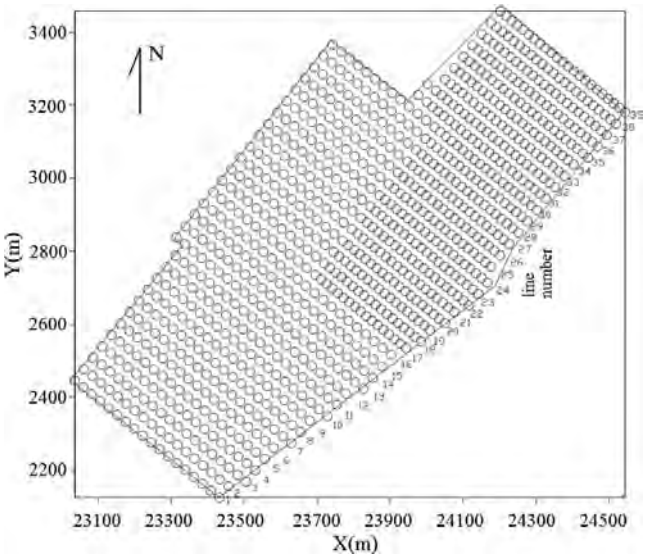

Figure 6. Layout of the survey area showing the 40 m by 10 m grid.

Based on the electrical exploration results (see Fig. 8(b)), a drilling location was selected adjacent to the location at 180 m on line 10. The depth of the borehole is 187.5 m. The drilling results verified the existence of a water-filled mine cavity at the depth of 130.25 m with a thickness of 5.1 m. The drilling result is consistent with the interpreted TEM results.

To outline the approximate range of the excavated cavity, a plan view of apparent resistivity contours at an altitude of 1,170 m is shown in Fig. 9(a). The figure shows that the distribution of resistivity is inhomogeneous. Many smaller regions exist corresponding to relatively low values in resistivity, likely to be mined-out areas filled with water. The geological interpretation is presented in Fig. 9(b). Four relatively large mined-out areas exist in the survey area. They are located in the center, northeast, and south (shaded areas).

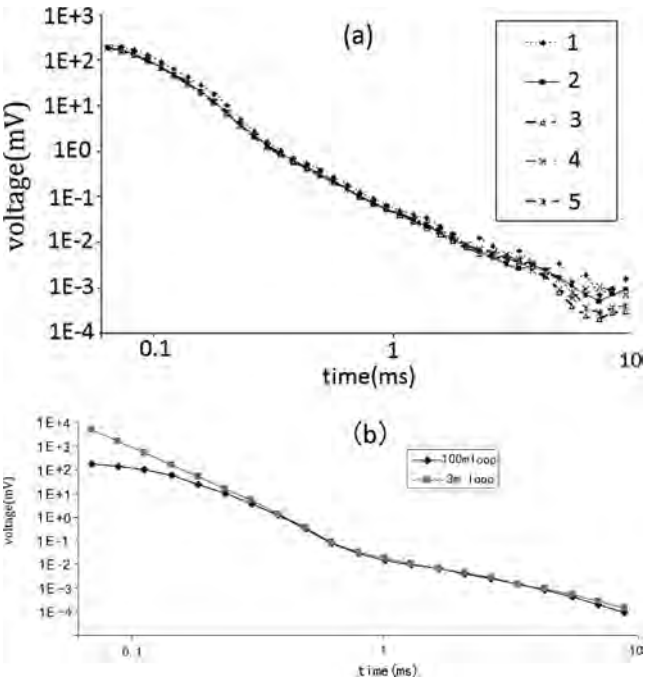

Figure 7. Testing and comparison survey using the EMRS-3 system. (a) Decay curves collected at the same location multiple times, showing the repeatability of the system. (b) Comparison between decay curves collected with the traditional loop (100 m × 100 m) Terra TEM system and EMRS-3 system.

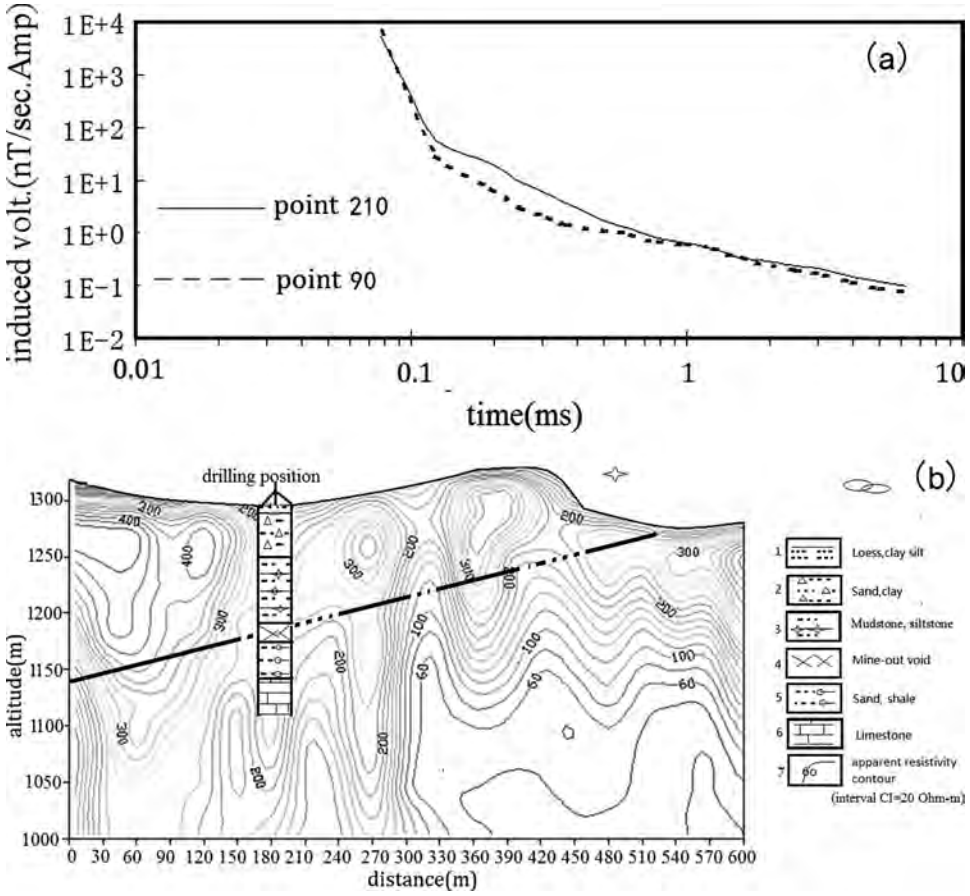

Figure 8. Survey result of line 10. a) Decay curve induced voltage at points 210 and 90 along line 10. b) Apparent resistivity contour map and interpreted result for line 10. The drilling result includes the water-filled mined-out space and coal seam. The dashed line connects the water-filled mine cavities at 0 m, 300–330 m, and 400–460 m.

Figure 10 shows three resistivity contour slice maps at depths of −150 m, −250 m, and −350 m. The white circle (low resistivity) areas represent the water-filled volumes. The lighter grey shaded areas (high resistivity) infer volumes without voids. Three boreholes were positioned in the water-filled areas. All of the drilling results are consistent with the TEM interpreted result.

Conclusions

The TEM method is sensitive to conductive subsurface features and useful for investigating water-filled cavities in coal mines. The detection depth of a TEM survey primarily depends on ground resistivity and diffusion time, relatively independent of transmitter loop size, which is consistent with Spies' (1989) opinion.

In practical exploration, a small loop source (3-m × 3-m loop) combined with a high power (1,000 A, 1,200 A) transmitter and a large equivalent area receiver coil in a central loop configuration can be used in mountainous areas.

The results and simulation show that: 1) in the early time, the response from the small loop model is higher than that from the large loop model; 2) in the late time, the responses of five different size loops are consistent, *i.e.*, all of them have theoretically the same deeper detecting depth; and 3) small loop sources are more sensitive to shallow targets.

A small transmitter loop system is more effective for shallow buried target mapping. The presented case study demonstrated the successful application of a high-powered small loop TEM system in mountains areas, identifying water-filled cavities in coal mines. The small loop system not only provides a useful alternative for TEM surveys, but also could be an option in other special survey conditions.

Acknowledgments

This work was supported by the National Nature Science Foundation (No.41174090, No. 41174108, No.

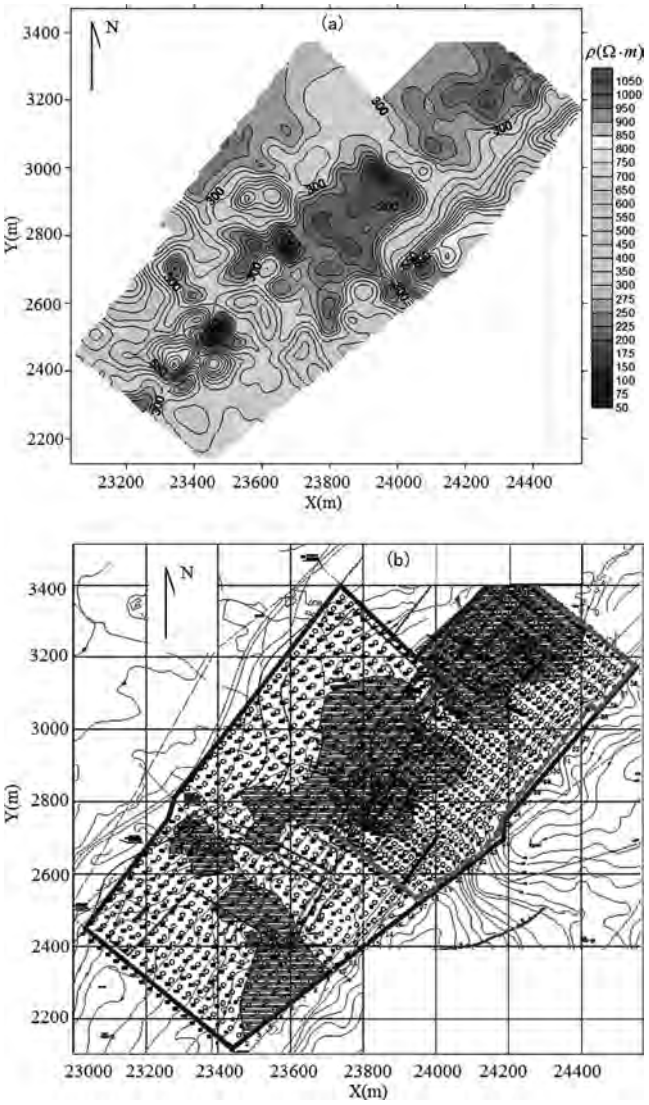

Figure 9. Plan views of apparent resistivity contour and interpreted result. a) Apparent resistivity contour map. b) Interpreted anomaly areas shown in black.

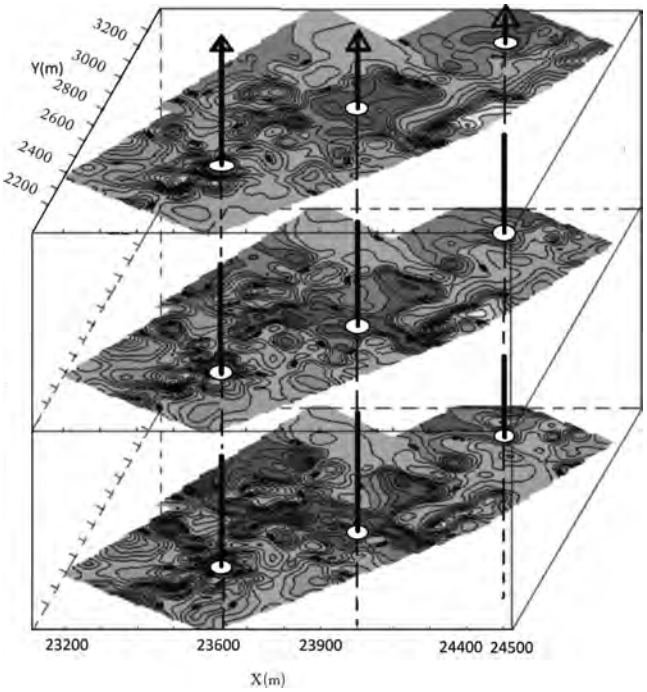

Figure 10. Apparent resistivity contour depth slices at −150 m, −250 m, and −350 m and borehole locations.

41130419). Many thanks to Professor Andrew Duncan, who is the managing director of electromagnetic imaging technology Pty Ltd (EMIT), for improving the English. The authors extend their gratitude to the editor and reviewers for their editorial suggestions.

References

Beard, L.P., 2011, Interpretation of out of loop data in large fixed-loop TEM surveys: *in* Expanded Abstracts: 81st Annual International Meeting, Society of Exploration Geophysicists, 18–23.

Guo, W.B., Xue, G.Q., Li, X., Quan, H.J., and Zhou, N.N., 2010, Study and application of the multiple small-aperture TEM system: Preview, **149**, 17–22.

Kaufman, A.A., and Keller, G.V., 1983, Frequency and transient sounding: Methods in geochemistry and geophysics: Elsevier Publ. Co, 1–32.

Nabighian, M.N., and Macnae, J.C., 1991, Time-domain electromagnetic prospecting methods: *in* Nabighian, M.N. (ed.), Electromagnetic methods in applied geophysics–Theory volume II, Part A, Society of Exploration Geophysicists, Tulsa, 427–520.

Oristaglio, M.L., and Hohmann, G.W., 1984, Diffusion of electromagnetic fields into a two dimensional earth: A finite-difference approach: Geophysics, **49**(7) 870–894.

Raiche, A.P., and Gallagher, R.G., 1985, Apparent resistivity and diffusion velocity: Geophysics, **50**(10) 1628–1633.

Singh, N.P., Utsugi, M., and Kagiyama, T., 2009, TEM response of a large loop source over a homogeneous earth model: A generalized expression for arbitrary source-receiver offsets: Pure and Applied Geophysics, **166**(12) 2037–2058.

Spies, B.R., 1980, Interpretation and design of time domain EM surveys in areas of conductive overburden: Bull. Austral. Soc. Expl. Geophys., **11**, 272–281.

Spies, B.R., 1989, Depth of investigation in electromagnetic sounding methods: Geophysics, **54**(7) 872–888.

Wang, T., and Hohmann, G.W., 1993, A finite-difference time-domain solution for three-dimensional electromagnetic modeling: Geophysics, **58**(6) 797–817.

Xue, G.Q., Qin, K.Z., Li, X., Li, G.M., Qi, Z.P., and Zhou, N.N., 2012a, Discovery of the large-scale porphyry molybdenum deposit in Tibet through modified TEM exploration method: Journal of Environmental and Engineering Geophysics, **17**(1) 19–25.

Xue, G.Q., Bai, C.Y., and Yan, Y., 2012b, Deep sounding TEM investigation method based on a modified fixed central-loop system: Journal of Applied Geophysics, **76**(2012) 23–32.

Xue, G.Q., and Li, X., 2012c, Physical simulation and application of a new TEM configuration: Environmental Earth Sciences, **67**(2012) 1291–1298.

Yan, S., Chen, M.S., and Shi, X.X., 2009a, Transient electromagnetic sounding using a 5m square loop: Exploration Geophysics, **40**(2) 193–196.

Yan, S., Shi, X.X., and Chen, M.S., 2009b, The probing depth of transient electromagnetic field method: Chinese Journal of Geophysics (in Chinese), **52**(6) 1583–1591.